p53 directly transactivates Δ133p53α, regulating cell fate outcome in response to DNA damage.

Jean-Christophe Bourdon, Mustapha Aoubala, Fiona Murray-Zmijewski, Marie P. Khoury, Kenneth Fernandes Fernandes, Stephane Perrier, Hugo Bernard, Anne-Catherine Prats, David P Lane

p53 directly transactivates Δ133p53α, regulating cell fate outcome in response to DNA damage.

Mustapha Aoubala[1]*, Fiona Murray-Zmijewski[1]*, Marie P. Khoury[1,2], Kenneth Fernandes[1], Stephane Perrier[1], Hugo Bernard[1,2], Anne-Catherine Prats[2], David P. Lane[1] and Jean-Christophe Bourdon[1,2‡].

[1]University of Dundee, College of Medicine, Centre for Oncology and Molecular Medicine, Inserm-European Associated Laboratory U858, Dundee, DD1 9SY, United-Kingdom.

[2]Unité mixte Inserm U858, Institut de Médecine Moléculaire de Rangueil, IFR 150, 1, Avenue Jean Poulhès, BP 84225, 31432 Toulouse Cedex 4, France.

* The first two authors contributed equally to this work.

Running title: Δ133p53-p53 is a new auto-regulatory feedback loop.

‡ Correspondence and requests for materials should be addressed to JC Bourdon
University of Dundee, College of Medicine, Centre for Oncology and Molecular Medicine, Inserm-European Associated Laboratory U858. Dundee, DD1 9SY, United-Kingdom.
Tel: +44 (0)1382496400
Fax: +44 (0)1382496363
(j.bourdon@dundee.ac.uk).

Author Information The authors declare no competing financial interest.

Abbreviations: p53RE: p53 responsive element; siRNA: small interfering RNA; siNS: non-specific siRNA; si133a: siRNA specific for Δ133p53 mRNAs; si133b: siRNA specific for Δ133p53 mRNAs; siTA: siRNA targeting specifically exon-2 of p53 mRNAs.

Abstract

We have previously reported that the human *p53* gene encodes at least nine different p53 isoforms, including Δ133p53α, which can modulate p53 transcriptional activity and apoptosis. In this study, we aimed to investigate the regulation of Δ133p53α isoform expression and its physiological role in modulating cell cycle arrest and apoptosis. We report here that in response to a low dose of doxorubicin (which induces cell cycle arrest without promoting apoptosis), p53 directly transactivates the human *p53* internal promoter, inducing Δ133p53α protein expression. The induced Δ133p53α then inhibits p53-dependent apoptosis and G1 arrest without inhibiting p53-dependent G2 arrest. Therefore, endogenous Δ133p53α does not exclusively act in a dominant-negative manner toward p53 but differentially regulates cell cycle arrest and apoptosis.

Introduction

The p53 tumor suppressor protein is a transcription factor that, in response to various forms of cellular stresses, regulates the expression of numerous genes involved in several biological activities such as cell cycle, apoptosis, differentiation and metabolism (1-3). The activation of p53 allows the preservation of the genome integrity and prevents genomic abnormalities being passed on to daughter cells, which could ultimately lead to cancer formation (3). The p53 protein itself is rapidly stabilized and activated in response to a wide variety of cellular stresses such as DNA damage, hypoxia, nutrient deprivation and viral infection. However, the ways by which the cell fate outcome is determined by p53 in response to different cellular stresses remain, to an extent, elusive (4). Furthermore, the molecular mechanisms by which p53 accomplishes its different activities are still not completely understood. So far, the best described mechanism is its ability to modulate gene expression by binding directly and specifically to p53 responsive elements (p53REs) on DNA (5).

It is now well established that the *p53* gene belongs to the same gene family as *p63* and *p73*, two other transcription factors that regulate transcription using similar responsive elements (p53REs) (6). Like most of the human genes, it has been shown that the *p63* and *p73* genes express multiple mRNA variants due to alternative splicing and usage of different promoters. Hence, genes encoding these two family members can express various isoforms of the p63 and p73 proteins which contain different domains of the protein(7). The *p53* gene was first thought to have a much simpler organization than the *p63* and *p73* genes, with transcription being initiated from two distinct sites upstream of exon-1 (P1 and P1') (7). We have assessed the structure of the *p53* gene, using a PCR-

based technique that specifically amplifies capped mRNAs (8). This showed that, similarly to p63 and p73, nine distinct human p53 protein isoforms (p53, p53β, p53γ, Δ40p53α, Δ40p53β, Δ40p53γ, Δ133p53α, Δ133p53β, Δ133p53γ) can be produced through alternative initiation of translation, usage of an internal promoter and alternative splicing (9). In this study, we refer to p53 as full-length p53 (FLp53). Expression of these different p53 isoforms, at the mRNA level, has been confirmed both in normal human tissues and in tumors (10-12). Moreover, the p53 isoforms have been shown to be differentially expressed in breast tumors, head and neck tumors, ovarian cancer, acute myeloid leukaemia, colorectal carcinoma and melanoma (10, 13-18). All this may suggest an important physiological function for the p53 isoforms.

We have previously shown that ectopic overexpression of Δ133p53α (an N-terminally truncated p53 isoform), negatively regulates p53 tumor suppressor activity by inhibiting p53-mediated apoptosis (8). Using the zebrafish animal model, we have recently reported that, in response to DNA-damaging agents and embryo development defects, the zebrafish *p53* internal promoter is induced by p53, leading to Δ113p53 protein expression (zebrafish homologue of human Δ133p53α), which prevents p53-mediated apoptosis (19). However, little is known about the molecular mechanisms by which human Δ133p53α modulates p53 activities at the physiological level.

In this study, we aimed to investigate the regulation of Δ133p53α expression and its physiological role in modulating the cellular response to DNA damage. Our results clearly show that the human *p53* internal promoter is directly transactivated by p53 in response to genotoxic stress, leading to Δ133p53α protein induction. The induced

Δ133p53α then inhibits p53-dependent apoptosis and G1 arrest, without inhibiting p53-dependent G2 arrest in U2OS cells. Our results further demonstrate that physiologically, Δ133p53α does not exclusively act in a dominant-negative manner toward p53 to differentially regulate cell cycle arrest and apoptosis.

Results

Mapping of the p53 internal promoter within intron-4 of the human p53 gene.

In the *p63* and *p73* genes, ΔN isoforms are transcribed from an internal promoter (P2), located within intron-3 of both genes (7). Although *p63* and *p73* are related to *p53*, no such internal promoter had been described for the *p53* gene. In our previous study, Gene-Racer PCR results showed that a transcription initiation site lies in the 3' end of intron-4 of the *p53* gene (8). Therefore, we sought to map the initiation site using deletion constructs within this region.

We first amplified by PCR a region of 1555 bp upstream of exon-5 of the human *p53* gene. This PCR fragment corresponding to nucleotides 11523-13076 of the human *p53* gene (accession no. X54156, NCBI), was cloned into the promoterless pGL3-basic plasmid, upstream of the firefly luciferase (luc) reporter gene, to generate the pi3i4-luc construct (Figure 1A, a). Subsequently, a number of deletion constructs (Figure 1A, b-f) of the recombinant pi3i4-luc construct were made by enzymatic digestion, followed by re-ligation or sub-cloning of fragments, as shown in Figure 1A.

To define the minimum promoter region, the different luciferase constructs were then transfected into p53-null H1299 cells (non-small cell lung carcinoma) and cell extracts were tested for luciferase activity. As shown in Figure 1B, the 1555 bp fragment (a) contains a promoter activity in H1299 cells. Its activity is similar to the basal promoter

activity of *Bax* and is approximately 4 times greater than the basal activity of the promoterless pGL3-basic plasmid. Deletion of residues 1 to 1304 (Figure 1A, constructs c, d and f) did not abolish the promoter activity (Figure 1B, c, d and f), suggesting that the minimum *p53* internal promoter region is located within the last 251 bp of the intron-4 (Figure 1A, f).

Moreover, the minimum *p53* internal promoter (Figure 1B, f) showed a significant increase in the basal promoter activity (4-fold), as compared to the basal activity of the pi3i4-luc construct (Figure 1B, a), suggesting that the region 1-1304 bp is likely to contain negative regulatory elements such as silencers. In fact, the basal promoter activity of the internal *p53* promoter (1304-1555, construct f) is increased (3-fold) compared to the basal promoter activity of the internal *p53* promoter (1042-1555, construct d), suggesting that the region 1042-1304 contains a silencer element. Bioinformatics analysis revealed that the *p53* internal promoter contains responsive elements to several transcription factors including p53, AP1, elk-1, ets, N-myc, E2F, HIF-1α, HSF1, ER, raising the possibility that it can be regulated by p53 and other transcription factors (Supplementary Figure A). Deletion of the last 251 bp from the 3' end of intron-4 (Figure 1A, constructs b and e) completely abolishes the promoter activity (Figure 1B, b and e), confirming that the initiation site of the *p53* internal promoter is located within the last 250 bp of intron-4 of the human *p53* gene.

Human Δ133p53 is a direct p53 target gene.

Using our bioinformatic software and our previously refined consensus p53RE (20), we investigated whether the *p53* internal promoter contains p53REs. The consensus p53RE

was defined as two consensus decamers (RRRCWWGYYY) flanked by at least two additional ones. A maximum of 3 differences to the consensus was accepted in total for the two consensus decamers, as well as for each additional decamer. Each additional decamer is allowed to bear one base insertion or deletion between the median C and G, if the two consensus decamers are contiguous. This set of criteria was validated by identifying within the promoter region of the *IGF-BP3* gene, the existence of a cluster of 11 decamers (p53REs) whose functional significance was verified (20). We identified five putative p53REs at the junction of exon-4 and intron-4 of the human *p53* gene corresponding to the residues 757-804 in the pi3i4-luc construct (Figure 2A, dashed box), suggesting that p53 may directly transactivate its own internal promoter.

To test this hypothesis, deletion constructs c and d (Figure 1A) were assessed for their responsiveness to p53 (Figure 2A, c and d respectively), in H1299 cells co-transfected with p53 expression vector and each of the generated luciferase constructs. A luciferase construct driven by the *p21* promoter was used as a positive control. As shown in Figure 2B, p53 induced the luciferase activity in all constructs containing the putative p53REs (Figure 2A, a and c). Interestingly, the greatest induction (6-fold) was obtained with the construct containing the 723-1555 bp fragment (Figure 2A, construct c), which contains all five p53REs but lacks the upstream 722 bp region of the *p53* internal promoter, suggesting that this region may contain negative regulatory elements. Interestingly, deletion of the five putative p53REs (Figure 2A, construct d) resulted in a significant decrease in p53 induction (Figure 2B, d compared to c). However, the induction by p53 of the promoter deleted of the region encompassing the p53REs (723-1042), (Figure 2B, d) is not totally abolished, suggesting that this region retains a weak responsiveness to

p53, either through direct DNA binding and/or interaction with other transcription factors or co-activators.

To further confirm that the putative identified sites correspond to p53REs, four single base mutations were generated by site-directed mutagenesis within the first two p53REs of the internal promoter. As shown in Figure 2C, the four mutations are sufficient to significantly decrease p53 transactivation of the entire *p53* internal promoter (construct a). This result clearly demonstrates that intron-4 of the *p53* gene contains functional p53REs. However, these mutations do not completely abolish p53 activation probably because of the presence of the remaining p53REs. Further analysis will be required to establish whether the remaining p53REs can confer responsiveness to p53.

Endogenous p53 can directly bind to and transactivate its internal promoter.

We next investigated whether endogenous p53 could directly bind to and transactivate its own internal promoter. MCF7 cells, (a breast cancer cell line expressing WTp53) were left untreated or treated with 60 ng/ml of Actinomycin D (Act D) for 2h and a chromatin immunoprecipitation (ChIP) assay was performed, using the mouse anti-p53 monoclonal antibody DO-1. The immunoprecipitated DNA was quantified by RT-qPCR (Figure 3A). A probe and primers specific for a region within the *GAPDH* gene that is not bound by p53, was used as a negative control. All GAPDH amplifications gave a cycle number greater than 40, indicating that no DNA was present in the ChIP samples and confirming the specificity of the assay. The binding of p53 to the *p21* promoter was analyzed as a positive control (Supplementary Figure B1). We further quantified the genomic DNA corresponding to either the p53REs (intron-4) or exon-8 of the *p53* gene, which is co-

immunoprecipitated with the p53 protein. As illustrated in Figure 3A, in unstressed cells, no significant binding of p53 to either intron-4 or exon-8 was observed. However, following Act D treatment, we observed an enhancement of the specific binding of endogenous p53 to intron-4 but not to exon-8. This clearly indicates that, in response to stress, endogenous p53 directly binds to its own internal promoter located within intron-4. RT-qPCR experiments were carried out in MCF7 and MCF7-DDp53 (a stable cell line overexpressing a dominant-negative form of p53) cells, to determine whether there is a p53-dependent induction of Δ133p53 mRNAs (Figure 3B). Since the PCR fragments corresponding to the Δ133p53 isoforms (Δ133p53α, Δ133p53β and Δ133p53γ) are all around 800 bp long and mRNA quantification by RT-qPCR is not reliable for large DNA fragments, it is not technically possible to specifically quantify each of the human Δ133p53 isoforms mRNAs. Therefore, we designed a probe and primers from the unique 5'UTR region of Δ133p53 mRNAs, encoding all three Δ133p53 isoforms (Δ133p53α, Δ133p53β and Δ133p53γ). MCF7 and MCF7-DDp53 cells were then treated with Act D. p21 mRNA induction was determined as a positive control (Supplementary Figure B2). As illustrated in Figure 3B, upon cellular stress, the expression of Δ133p53 mRNAs is significantly induced 2h following Act D treatment. No induction of p21 or Δ133p53 mRNAs was seen in MCF7-DDp53 cells, confirming that the induction of Δ133p53 mRNAs is p53-dependent**.**

To assess whether Δ133p53 mRNAs induction could occur in other cell lines and in response to other DNA-damaging agents, we compared the expression of Δ133p53 mRNAs in response to doxorubicin treatment in colorectal carcinoma cell lines, expressing WTp53 (HCT116+/+) or devoid of FLp53 expression (HCT116-/-). In

HCT116-/- cells, the *neomycin* gene has been integrated within exon-2 of the *p53* gene, resulting in the loss of FLp53 expression (21). However, HCT116-/- cells still express p53 isoforms at the mRNA and protein levels, due to initiation of translation from codon 40 located in exon-4 of the *p53* gene (9, 22). We show here that Δ133p53 mRNAs are inducible in response to doxorubicin only in HCT116+/+ but not in HCT116 -/- cells (Figure 3C). Similar results were obtained in response to etoposide treatment (data not shown). We further investigated Δ133p53 mRNAs induction after treating U2OS osteosarcoma cell line (expressing WTp53) and primary normal human dermal fibroblasts (NHDF) with doxorubicin (Figure 3D and 3E, respectively). Similarly to MCF7 and HCT116+/+ cells, Δ133p53 mRNAs expression is significantly induced upon doxorubicin treatment in both cell lines. The data indicate that induction of Δ133p53 mRNAs expression is p53-dependent in multiple cell lines. Altogether, these results demonstrate that *in vivo*, the *p53* internal promoter located within intron-4, is directly transactivated by p53 in response to DNA damage

Δ133p53α protein expression is induced by p53 in response to DNA damage.

Western blot analyses were performed to determine whether the increase of Δ133p53α protein is associated with the expression of Δ133p53 mRNAs. The rabbit polyclonal antibody CM1 was raised against full-length recombinant human p53 protein and can detect all p53 protein isoforms, including Δ133p53α. We thus analyzed Δ133p53α protein expression in HCT116+/+ and HCT116-/- cells, treated or not with doxorubicin. To prevent any *in vitro* protein degradation, cells were directly lyzed in SDS-Laemmli buffer. The results in HCT116+/+ cells show that doxorubicin treatment clearly induces

p53 and some p53 isoforms migrating at 48 kD, 45 kD and 35 kD (Figure 4A). In HCT116-/- cells, a strong expression of Δ40p53 was detected but neither Δ40p53 nor other p53 isoforms were induced in response to doxorubicin treatment. However, it is not technically possible with the CM1 antibody to specifically identify the Δ133p53α isoform by western blot analysis. Therefore, we designed two distinct siRNAs (si133a and si133b) specific for the Δ133p53 isoforms (Δ133p53α, Δ133p53β and Δ133p53γ), which target the 5'UTR of Δ133p53 mRNA variants. The specificity and efficiency of the designed siRNAs were first assessed by RT-qPCR analysis in U2OS cells (Supplementary Figure C1).

Having confirmed the specificity and efficiency of the Δ133p53 siRNAs (si133a or si133b), we then attempted to identify by western blot the bands corresponding to endogenous Δ133p53α protein in HCT116 cells, transfected with either si133a, si133b or siNS as a negative control (Figure 4B). Doxorubicin treatment induced the expression of p53 and also of some p53 isoforms migrating at 48 kD, 45 kD and 35 kD (Figure 4B lane 5 compared to 1). The two Δ133p53 siRNAs, si133a and si133b, did not alter the level of endogenous p53 or of the other p53 isoforms (corresponding to the bands at 48 kD, 45 kD) but specifically reduced the expression of the 35 kD band (Figure 4B, lanes 4, 6 compared to 5), indicating that the 35kD band corresponds to endogenous Δ133p53α protein.

The induction of Δ133p53α protein was further confirmed by western blot analysis in primary normal human dermal fibroblasts (NHDF) treated with doxorubicin (Figure 4C). Altogether, these results demonstrate that, in the cancer derived cell lines (HCT116

WTp53) and in the normal primary fibroblasts, Δ133p53α isoform is induced by p53 at both mRNA and protein levels in response to DNA damage.

Generation and characterization of U2OS-ctrl and U2OS-Δ133p53 cells.

To determine the role of Δ133p53α in the cellular response to DNA damage, we investigated by BrdU cell cycle analysis and apoptosis assay (annexinV assay) the experimental conditions which enable the U2OS cells to undergo cell cycle arrest rather than apoptosis, in response to doxorubicin. We established that U2OS cells grown for 24h at 50% confluence and treated with a low dose of doxorubicin (0.5μM for 1h), trigger G2 cell cycle arrest without promoting apoptosis 24h after treatment. Those experimental conditions were then used in all the following experiments.

Two cellular models were generated in order to define the biological relevance of Δ133p53α induction in response to DNA damage. U2OS cells were stably transfected with the empty pcDNA3 or pcDNA3-Δ133p53α expression vectors, to generate U2OS-ctrl and U2OS-Δ133p53 cells respectively. U2OS-Δ133p53 cells were used to assess whether the biological effects of Δ133p53 mRNAs depletion by si133a or si133b could be rescued by restoration of Δ133p53α expression.

First, we analyzed ectopic Δ133p53α protein expression in U2OS-Δ133p53 cells by western blot analysis, using the CM1 antibody (Figure 5A). U2OS-Δ133p53 cells transfected with either si133a, si133b or siNS were left untreated or treated with doxorubicin (0.5μM, 1h). As shown in Figure 5A, lane 1, ectopic Δ133p53α protein was expressed at 35kD. A weaker band at 32kD could also be detected and may correspond to a post-translationally modified form of Δ133p53α. Transfection of U2OS-Δ133p53 cells

with si133a or si133b specifically knocked-down the bands at 35kD and 32kD corresponding to ectopic Δ133p53α protein, without affecting p53 protein level (Figure 5A, lanes 2, 3 compared to 1). In U2OS-Δ133p53 cells, doxorubicin treatment induced p53 protein expression but had no detectable effect on Δ133p53α protein expression (Figure 5A, lane 4 compared to 1). This is because the ectopic expression of Δ133p53α, driven by the *CMV* promoter (pcDNA3 plasmid), is largely above the endogenous expression level and therefore masks the induction of endogenous Δ133p53α (Figure 5B lane 1 compared to 7). Depletion of Δ133p53α by si133a or si133b was equally efficient in doxorubicin-treated and untreated U2OS-Δ133p53 cells (Figure 5A, lanes 2, 3 compared to 1 and lanes 5, 6 compared to 4). The induction of p53 in response to doxorubicin is comparable in U2OS-Δ133p53 cells transfected with either si133a, si133b or siNS (Figure 5A, lanes 5, 6 compared to 4). This clearly shows that p53 can be induced in U2OS-Δ133p53 cells in response to doxorubicin treatment.

To compare the expression level of Δ133p53α protein in U2OS-ctrl and U2OS-Δ133p53 cells, the same amount of protein from U2OS-Δ133p53 cells was loaded in Figure 5A, lane 1 and in Figure 5B, lane 1. Endogenous Δ133p53α protein was not detectable in untreated U2OS-ctrl cells (Figure 5B, lanes 2, 3). Transfection of si133a or si133b did not affect the expression of p53 in untreated U2OS-ctrl cells (Figure 5B, lanes 4,5). In response to doxorubicin (0.5μM, 1h), endogenous Δ133p53α was induced in U2OS-ctrl cells (Figure 5B, lane 3 compared to 7). Of note, in U2OS-ctrl cells treated with doxorubicin, endogenous Δ133p53α protein level is far below the expression levels of ectopic Δ133p53α protein in U2OS-Δ133p53 cells (Figure 5B lane 7 compared to 1). Transfection of U2OS-ctrl cells with si133a or si133b inhibited the induction of

endogenous Δ133p53α protein in response to doxorubicin (Figure 5B, lanes 8, 9 compared to 7). To determine whether the induction of Δ133p53α in doxorubicin-treated U2OS-ctrl cells is p53-dependent, cells were transfected with siTA, an siRNA that specifically targets p53 mRNAs containing exon-2 of the *p53* gene (p53, p53β, p53γ, Δ40p53α, Δ40p53β and Δ40p53γ), without targeting Δ133p53 mRNAs. The results show that Δ133p53α protein induction is inhibited in doxorubicin-treated U2OS-ctrl cells depleted of p53 expression, confirming that Δ133p53α is induced by p53 (Figure 5B, lane 6 compared to 7).

Human Δ133p53α antagonizes p53-mediated apoptosis and G1 cell cycle arrest without preventing G2 cell cycle arrest.

We next investigated whether the cellular response to DNA damage could be regulated by modulating Δ133p53α expression. U2OS-ctrl and U2OS-Δ133p53 cells were transfected with either si133a, si133b or siNS and were left untreated or treated with doxorubicin (0.5μM, 1h) for 24h. In parallel to the western blots presented in Figures 5A and 5B, cell cycle progression (Figures 5C, 5D and 5E) and apoptosis (Figure 5F) were analyzed by BrdU assay and Annexin-V assay respectively. A representative BrdU experiment is shown in Figure 5C. Untreated U2OS-ctrl and U2OS-Δ133p53 cells transfected with siNS showed similar cell cycle progression and a low percentage of spontaneous apoptosis (8%), indicating that overexpression of Δ133p53α does not alter cell cycle progression and apoptosis in untreated cells (Figures 5C-a, 5C-b, 5D, 5E and 5F). Similar results were obtained in untreated and untransfected cell lines.

U2OS-ctrl and U2OS-Δ133p53 cells transfected with siNS and treated with a low dose of doxorubicin show statistically similar cell cycle progression with about 3% of cells arrested in G1 and 79% of cells arrested in G2 (Figures 5C-c, 5C-d and 5E). In both cell lines, the low dose of doxorubicin did not significantly increase apoptosis compared to untreated cells (Figure 5F). Altogether, this indicates that overexpression of Δ133p53α in U2OS-Δ133p53 cells does not alter the cellular response to a low dose of doxorubicin, compared to U2OS-ctrl cells (Figures 5C-c, 5C-d, 5D, 5E and 5F). To determine whether spontaneous apoptosis and the induction of G2 cell cycle arrest in response to a low dose of doxorubicin is p53-dependent, U2OS-ctrl cells were transfected with siTA. We detected a statistically significant decrease in the percentage of cells arrested in G2 (Figure 5E) and in the percentage of apoptotic cells, compared to U2OS-ctrl cells transfected with siNS and treated with a low dose of doxorubicin (Figure 5F). This is consistent with previous publications reporting that doxorubicin induces G2 cell cycle arrest and apoptosis in a p53-dependent manner in U2OS cells (23). As we have previously reported that overexpression of Δ133p53α can act in a dominant negative manner toward p53 (8, 9), it is surprising that the overexpression of Δ133p53α in U2OS-Δ133p53 cells does not inhibit p53-mediated G2 arrest. It implies that Δ133p53α does not exclusively act in a dominant-negative manner toward p53.

Strikingly, in response to doxorubicin treatment, depletion of the Δ133p53 isoforms with si133a or si133b significantly enhanced the percentage of U2OS-ctrl cells in G1 arrest (16% and 26% respectively, Figures 5C-e and 5D), suggesting that endogenous Δ133p53α inhibits G1 cell cycle arrest in U2OS-ctrl cells. To confirm that the G1 arrest is due to the specific depletion of Δ133p53α and not to off-target effects of the siRNAs,

U2OS cells overexpressing Δ133p53α (U2OS-Δ133p53) were transfected with si133a or si133b. Although both siRNAs inhibit Δ133p53α expression in U2OS-Δ133p53 cells, Δ133p53α protein level was still overexpressed compared to endogenous Δ133p53α protein level in U2OS-ctrl cells (Figure 5A). The results showed that transfection of si133a or si133b in U2OS-Δ133p53 does not significantly change the percentage of cells in G1 in response to a low dose of doxorubicin (Figure 5C-f and 5D), confirming that si133a and si133b are specific and that Δ133p53α inhibits G1 arrest in U2OS-ctrl cells. Of note, no statistically significant alteration in the percentage of cells in S phase was observed (Figure 5C).

Regarding apoptosis (Figure 5F), in U2OS-ctrl cells transfected with si133a or si133b and compared to cells transfected with siNS, a statistically significant increase in the percentage of apoptotic cells was detected, suggesting that a low dose of doxorubicin can trigger apoptosis if cells are depleted of Δ133p53α. Consistent with this, in U2OS-Δ133p53 cells transfected with si133a or si133b and compared to cells transfected with siNS, a statistically significant lower increase in the percentage of apoptotic cells was observed in response to a low dose of doxorubicin. This indicates that overexpression of Δ133p53α rescued the resistance to apoptosis in response to a low dose of doxorubicin confirming that endogenous Δ133p53α inhibits p53-mediated apoptosis in U2OS-ctrl cells.

Altogether, our results show that in response to a low dose of doxorubicin, endogenous Δ133p53α antagonizes p53-mediated apoptosis and G1 arrest, without inhibiting p53-dependent G2 arrest. This indicates that Δ133p53α does not exclusively inactivate

p53. Moreover, it demonstrates that the cellular response to DNA damage could be regulated by modulating Δ133p53α expression.

Human Δ133p53α *can form a protein complex with p53 and can differentially regulate p21*, *HDM2* and *Bcl-2 expression in response to stress.*

We have previously reported that ectopic Δ133p53α can act in a dominant-negative manner toward p53 (9). In order to explain the regulation of p53 activities by Δ133p53α, we investigated whether Δ133p53α could directly interact with p53. Co-immunoprecipitation assays were carried out on p53-null H1299 cells transfected with Δ133p53α and/or p53, using the mouse monoclonal antibody DO-1, recognising FLp53 but not Δ133p53α. Immunoprecipitated proteins were then analyzed by western blot with the rabbit polyclonal antibody (CM1), recognizing FLp53 and Δ133p53α. The results clearly show that Δ133p53α can form a protein complex with p53 (Figure 6A).

We then studied whether endogenous Δ133p53α could regulate p53 target gene expression in response to DNA damage. In this study, we focused our investigation on a few p53 target genes (*p21*, *HDM2* and *Bcl-2*), implicated in cell cycle progression and apoptosis. *p21* encodes a cyclin-dependent kinase inhibitor involved in G1 and G2 cell cycle arrest (24), while HDM2 is an E3-ubiquitin ligase that regulates p53 protein degradation (25, 26). Both *p21* and *HDM2* genes are directly transactivated by p53 in response to stress, whereas *Bcl-2* is an anti-apoptotic gene repressed by p53 (27) (28).

Their expression was determined by western blot analysis (Figure 6B), using protein extracts from U2OS-ctrl cells analyzed in Figure 5B. RT-qPCR analysis was also performed in parallel (Supplementary Figure D). Doxorubicin treatment induced the

expression of p21 and HDM2 at the mRNA and protein levels but had no effect on Bcl-2 expression (Supplementary Figure D and Figure 6B lane 2 compared to 1). Depletion of FLp53 by siTA after doxorubicin treatment strongly inhibited p21 and HDM2 at the mRNA and protein levels, without having an effect on Bcl-2 expression (Supplementary Figure D and Figure 6B lane 5 compared to 2). This confirms that in U2OS-ctrl cells, induction of p21 and HDM2 expression in response to a low dose of doxorubicin is p53-dependent, while it suggests that Bcl-2 expression in U2OS-ctrl cells is not p53-dependent. Then, we compared to siNS, the effect of Δ133p53α depletion by si133a or si133b on the expression of p21, HDM2 and Bcl-2, in cells treated with doxorubicin (Supplementary Figure D and Figure 6B lanes 3, 4 compared to 2). Depletion of Δ133p53α significantly increased the expression of p21 mRNA but did not alter p21 protein expression. Interestingly, Δ133p53α depletion reduced the expression of HDM2 and Bcl-2 at both protein and mRNA levels. This suggests that Δ133p53α can increase Bcl-2 expression and contributes to the induction of HDM2 expression, in response to a low dose of doxorubicin. Therefore, our results show that Δ133p53α can differentially regulate p21, HDM2 and Bcl-2 expression and that Δ133p53α can directly interact with p53.

Altogether, we show that p53-mediated expression of Δ133p53α in response to a low dose of doxorubicin, leads to the inhibition of p53-mediated apoptosis and G1 cell cycle arrest without impairing p53-mediated G2 cell cycle arrest. Moreover, we show that Δ133p53α can directly interact with p53 and can differentially regulate the expression of

p21, HDM2 and Bcl-2 in response to a low dose of doxorubicin. This indicates that Δ133p53α does not exclusively inhibit p53 but rather modulates p53 activities.

Discussion

We have recently reported that the human *p53* gene encodes nine different p53 isoforms, two of which can modulate p53 transcriptional activity and apoptosis. We have previously shown that p53β and Δ133p53α isoforms can modulate p53 target gene expression, in a promoter-dependent manner. In addition, we have reported that ectopic overexpression of the N-terminally truncated isoform Δ133p53α inhibits p53-mediated apoptosis (8). In this report, we investigated the regulation of *p53*'s internal promoter within intron-4 of the *p53* gene, and the biological activities of endogenous Δ133p53α in response to a low dose of doxorubicin.

We determined that the initiation site of the *p53* internal promoter is located within the last 250 bp of intron-4. Moreover, we identified five putative p53REs at the junction of exon-4 and intron-4 of the human *p53* gene. By ChIP assay, luciferase reporter assay and site-directed mutagenesis, we showed that p53 binds directly to the p53REs and thus transactivates its own internal promoter in response to doxorubicin treatment. Further analysis will be required to establish whether all five p53REs can confer responsiveness to p53. It would be interesting to determine whether the *p53* internal promoter can be regulated by p63 and/or p73. By bioinformatics analysis, we determined that the *p53* internal promoter contains also numerous responsive elements to transcription factors that promote cell proliferation (AP1, Elk1, N-myc, E2F), are responsive to hypoxia (HIF-1α), to heat shock (HSF1) or to hormones (estrogen receptor). In addition, we identified a

silencer region (position 1042-1304) within the *p53* internal promoter suggesting that it can also be repressed by other transcription factors (ZNF219, CBF1). Therefore, the *p53* internal promoter is responsive to stress and proliferation signals which would regulate p53 tumour suppressor activity by modulating Δ133p53α expression.

To date, it is still technically difficult to specifically quantify by RT-qPCR large DNA fragments. Therefore, it was not possible for us to design primers and probe sets to specifically quantify the expression of each separate Δ133p53 isoform (Δ133p53α, Δ133p53β and Δ133p53γ), encoded from the *p53* internal promoter. Hence, to quantify at the mRNA level the expression of the Δ133p53 isoforms (Δ133p53α, Δ133p53β and Δ133p53γ), we designed primers and probe specific for the 5'UTR of Δ133p53 mRNAs, which is not present in FLp53 mRNA. We then showed that the human *p53* internal promoter is induced in response to doxorubicin or Actinomycin D treatment, in different cancer derived cell lines expressing WTp53 (HCT116, U2OS and MCF7), as well as in primary normal human fibroblasts (NHDF). This indicates that the induction of the *p53* internal promoter is not specific for cancer cells. By comparing Δ133p53 mRNAs expression in response to DNA damage in MCF7 (WTp53) and MCF7-DDp53 (overexpressing dominant negative p53 form) cells or in HCT116+/+ (WTp53) and HCT116-/- cells (devoid of FLp53 expression), we showed that the activation of the *p53* internal promoter leading to Δ133p53 mRNAs expression is p53-dependent in response to DNA damage. This is consistent with our recent report on the induction of zebrafish *p53* internal promoter by p53 in response to DNA-damaging agents, suggesting that p53-mediated regulation of its own internal promoter is conserved through evolution (19). Moreover, *p63* and *p73* internal promoters, which respectively lead to ΔNp63 and ΔNp73

expression, are also regulated by full-length p63 and p73 (7). Therefore, the regulation of *p53*/*p63*/*p73* internal promoters respectively by p53, p63 and p73 is a feedback-loop conserved among the *p53* gene family, suggesting that the regulation of *p53*/*p63*/*p73* internal promoters plays an important role in the biological activities of the p53 family members. It is worth noting that the *p53* internal and the *p53* proximal promoters are distinct, therefore the ratio of these isoforms could be independently modulated in a tissue-specific manner and in response to different stresses.

Western blot analyses were performed to determine whether the expression of Δ133p53 mRNAs is associated with an increase of Δ133p53α protein level. The rabbit polyclonal antibody CM1, which was raised against full-length recombinant human p53 protein, has a strong affinity for p53, recognizing several epitopes in the N-terminal and C-terminal domains of p53. CM1 can thus detect all forms of the p53 protein, including Δ133p53α (Figures 4 and 5). However, we would like to point out that it is not possible to compare the expression level of Δ133p53α with p53 protein by western blot analysis using the CM1 antibody, since the N-terminal domain of p53, which contains most of the CM1 epitopes, is not present in the Δ133p53α protein. Therefore, the CM1 antibody does not detect Δ133p53α as efficiently as the p53 protein.

We showed by western blot that doxorubicin treatment induces accumulation of the p53 protein and its isoforms in HCT116+/+, U2OS and NHDF cells but not in HCT116-/- cells, devoid of FLp53 expression. To identify the band corresponding to the Δ133p53α isoform, we inhibited its expression with two distinct siRNAs (si133a and si133b), specific for the 5'UTR of the Δ133p53 mRNA variants. We determined that endogenous Δ133p53α protein corresponds to a band at 35 kD induced in response to DNA damage

in HCT116+/+ and U2OS cancer cells, as well as in primary NHDF, indicating that the induction of the Δ133p53α protein is not specific for cancer cells. Of note, ectopic and endogenous Δ133p53α give a band at 35kD and a weaker band at 32kD, in U2OS cells. We assume that the band at 32 kD corresponds to a post-translationally modified form of Δ133p53α and we are currently characterizing its origin.

We then investigated the biological relevance to Δ133p53α induction in response to DNA damage. We have recently published that Δ113p53, the zebrafish homologue of human Δ133p53α, prevents p53-mediated apoptosis in response to embryonic defects or DNA damage (19) and that human Δ133p53α can inhibit replicative senescence (18). Here, we investigated whether the cellular response to DNA damage could be regulated by modulating Δ133p53α expression. In this aim, we explored the experimental conditions inducing p53-mediated cell cycle arrest without promoting p53-mediated apoptosis, in response to doxorubicin treatment. We determined that treatment of U2OS-ctrl cells with a low dose of doxorubicin (0.5μM, 1h) induces exclusively p53-dependent G2 cell cycle arrest without promoting G1 cell cycle arrest or p53-dependent apoptosis. Then, we established that the cellular response to the same dose of doxorubicin can be changed by regulating Δ133p53α expression. Indeed, U2OS-ctrl cells depleted of Δ133p53 mRNAs by si133a or si133b and treated with doxorubicin (0.5μM, 1h) increases the proportion of cells undergoing apoptosis and G1 cell cycle arrest. Overexpression of Δ133p53α restores resistance to apoptosis and abolition of G1 cell cycle arrest without preventing p53-mediated G2 cell cycle arrest. The inhibition of p53-mediated apoptosis and G1 cell cycle arrest in response to Δ133p53α expression is consistent with our previous reports showing that Δ133p53α can act in a dominant-

negative manner toward p53 (8, 9, 18). The direct interaction of Δ133p53α with p53 is in support of this mechanism. However, as the overexpression of Δ133p53α did not inhibit p53-dependent G2 cell cycle arrest in response to doxorubicin treatment, it indicates that Δ133p53α does not exclusively act by inactivating p53. This is confirmed by the fact that *p21*, *Bcl-2* and *HDM2* genes are differentially regulated by Δ133p53α in response to DNA damage. Δ133p53α represses p21, while it induces Bcl-2 and HDM2 expression. The repression of p21 is consistent with a dominant-negative effect of Δ133p53α toward p53. However, as Δ133p53α is required for HDM2 induction, it confirms that Δ133p53α does not exclusively act by inactivating p53. It suggests that many genes are differentially regulated by Δ133p53α to modulate cell fate outcome in response to DNA damage. Regulation of gene expression is complex and involves transcriptional and post-transcriptional pathways. Further experiments will be required to identify the genes regulated by Δ133p53α and decipher the role of Δ133p53α in the regulation of each of those genes. Our findings may have profound significance to extend our understanding of the mechanisms by which p53 exerts its tumor suppressor activity. They demonstrate a new feedback loop in which p53-induced Δ133p53α acts to modulate the cellular response to DNA damage.

Acknowledgements

Mustapha Aoubala is supported by Breast Cancer Campaign, Fiona Murray-Zmijewski was supported by Breast Cancer Campaign and MRC. Marie P. Khoury and Stephane Perrier are supported by Inserm (Institut National de la Santé Et de la Recherche Médicale), Hugo Bernard is supported by Ligue Nationale Contre le Cancer. Kenneth Fernandes and Jean-Christophe Bourdon are supported by Cancer-Research UK. The authors wish to thank Drs Mark Saville and Alice Marchado-Silva for their constructive discussions.

Materials and Methods

p53 internal promoter constructs

The *p53* internal promoter, corresponding to the region 11523-13076 bp of the human *p53* gene (accession no. X54156, NCBI), was generated by PCR using the primers p53RE-a fwd and p53RE-a rev (Table-1). The PCR fragment was first cloned into the pCR®4-TOPO® vector using the TOPO TA Cloning® kit (Invitrogen) and was further sub-cloned into the pGL3-basic plasmid, upstream of the luciferase reporter gene, to generate the pi3i4-luc construct (construct a in Figure 1A). Subsequently, a number of deletion constructs of pi3i4-luc (b, c, d and e in Figure 1A) were made by enzymatic digestion using various restriction enzymes, followed by re-ligation and sub-cloning of the obtained fragments. Two other pi3i4-luc constructs (constructs c and d in Figure 2A), with or without p53REs, were generated by PCR using the primers' combination p53RE-b fwd/p53RE-a rev and p53RE-c fwd/p53RE-a rev for constructs b and c, respectively (Figure 2A and Table-1). Site-directed mutagenesis of the identified p53REs was carried out by PCR on the pi3i4-luc, using the primers Mut-p53RE fwd and Mut-p53RE rev (Table-1). All generated constructs were verified by DNA sequencing.

Dual luciferase assay

H1299 cells ($3x10^4$) were seeded in 24-well plates, 24 hours prior to transfection. Two hours before transfection, media was replaced with 0.5 ml of fresh complete DMEM. Each transfection was performed in duplicate, and all results shown are the average of at least three separate individual experiments. For each well, 0.5 μg of each p53 internal promoter construct (as indicated in the legends) and 50 ng of the Renilla luciferase

reporter plasmid were co-transfected with 200 ng of the FLp53 expression vector or with the pSI (empty expression vector), used as negative control. The Renilla luciferase reporter plasmid was used as an internal control. Luciferase assays were performed as previously described (29).

Cell culture and generation of stable cell lines

The different human cell lines used in our study were: the non small lung carcinoma cell line H1229 (p53-null), the osteosarcoma cell line U2OS (WTp53), The colon cell lines HCT116 (WTp53), the breast cancer cell line MCF7 (WTp53) and the primary normal human dermal fibroblasts NHDF. The MCF7 stable line overexpressing a dominant negative form of p53 (MCF7-DDp53) (30) was also used. The HCT116 -/-, devoid of FLp53 expression, were kindly provided by Pr. Vogelstein's lab (21). Two U2OS stable cell lines were generated after transfection with either the empty pcDNA-3 expression vector (U2OS-ctrl) or with the pcDNA3-Δ133p53 expression vector (U2OS-Δ133p53). The heterogeneous populations of both cells lines were used in the experiments, no clones were isolated. NHDF cells were kindly provided by Dr C. Pourreyron. H1299 cells were cultured in RPMI medium supplemented with 10% fetal calf serum and 100 μg/ml penicillin/streptomycin. All the other cell lines were cultured in DMEM medium supplemented with 10% fetal calf serum and 100 μg/ml penicillin/streptomycin.

RNA extraction, cDNA synthesis, RT-qPCR and Chromatin Immunoprecipitation (ChIP) Assay

Total RNA was extracted with the RNeasy Mini Kit (Qiagen) and treated with DNase (Qiagen) prior to reverse transcription, which was carried out using random hexamers (Promega) and Superscript II reverse transcriptase (Invitrogen). qPCR was performed on Stratagene MX3005P. p53 specific primers and probes were designed in our laboratory (Table-1) and purchased from MWG. RT-qPCR analyses for the *p21*, *Bax*, *HDM2* and *Bcl2* genes were performed as previously described (31, 32). All measurements were normalized to the expression of the TATA box-binding protein (*TBP*) gene. p53 specific ChIP assay was conducted on MCF7 cells, as previously described using anti-p53 monoclonal antibody, DO1 (8) .

Western blot analysis

Cells lysates were separated by 4-12% SDS PAGE (Novagen system), transferred to a nitrocellulose membrane and blotted with various antibodies. The primary antibodies used were the following: anti-p53 CM1 (33), anti-HDM2 4B2 (31), p21 (Calbiochem), PARP (Roche), Bax, Bcl2 and actin (Santa Cruz). All secondary Horseradish peroxidase (HRP) conjugated antibodies were purchased from Jackson ImmunoResearch Laboratories.

Immunoprecipitation assay

H1299 (10^6 cells/10-cm dish) were co-transfected with 2µg pSV-p53 expression vector driven by the *SV40* promoter and/or 2µg pSV-Δ133p53 expression vector driven by the *SV40* promoter. For each transfection mix, the concentration of the *SV40* promoter was balanced with the *SV40* empty expression vector. Fugene (Boehringer) was used as a

transfection reagent. Immunoprecipitation was carried out as previously described (8) with anti-p53 mouse monoclonal antibody DO-1.

Protein content was then analyzed by western blot with anti-p53 rabbit polyclonal antibody (CM1), as previously described (8).

Small interfering RNA (siRNA) transfection, Apoptosis and Cell cycle analyses

U2OS (10^5 cells/6-well plate) were transfected with the appropriate siRNA using oligofectamine (Invitrogen), treated with doxorubicin and further incubated for 24h before harvesting for apoptosis and cell cycle assays. The efficiency of si133a, si133b and siTA was assessed by RT-qPCR (Supplementary Figures C1 and C2). Apoptotic cells were quantified using an Annexin V-fluorescein isothiocyanate kit (Biosciences), according to the manufacturer's instructions and were analyzed by flow cytometry (Becton Dickinson). Cell cycle analysis was carried out using BrdU (bromodeoxyuridine, Sigma) pulse labeling and flow cytometry, as previously described (34) and according to the manufacturer's instructions.

1. Royds JA, Iacopetta B. p53 and disease: when the guardian angel fails. *Cell Death Differ* 2006 Jun; **13** (6)**:** 1017-1026.

2. Braithwaite AW, Prives CL. p53: more research and more questions. *Cell Death Differ* 2006 Jun; **13** (6)**:** 877-880.

3. Vousden KH, Lane DP. p53 in health and disease. *Nat Rev Mol Cell Biol* 2007 Apr; **8** (4)**:** 275-283.

4. Lavin MF, Gueven N. The complexity of p53 stabilization and activation. *Cell Death Differ* 2006 Jun; **13** (6)**:** 941-950.

5. Laptenko O, Prives C. Transcriptional regulation by p53: one protein, many possibilities. *Cell Death Differ* 2006 Jun; **13** (6)**:** 951-961.

6. Mondal N, Parvin JD. The tumor suppressor protein p53 functions similarly to p63 and p73 in activating transcription in vitro. *Cancer Biol Ther* 2005 Apr; **4** (4)**:** 414-418.

7. Moll UM, Slade N. p63 and p73: roles in development and tumor formation. *Mol Cancer Res* 2004 Jul; **2** (7)**:** 371-386.

8. Bourdon JC, Fernandes K, Murray-Zmijewski F, Liu G, Diot A, Xirodimas DP*, et al.* p53 isoforms can regulate p53 transcriptional activity. *Genes Dev* 2005 Sep 15; **19** (18)**:** 2122-2137.

9. Murray-Zmijewski F, Lane DP, Bourdon JC. p53/p63/p73 isoforms: an orchestra of isoforms to harmonise cell differentiation and response to stress. *Cell Death Differ* 2006 Jun; **13** (6)**:** 962-972.

10. Boldrup L, Bourdon JC, Coates PJ, Sjostrom B, Nylander K. Expression of p53 isoforms in squamous cell carcinoma of the head and neck. *Eur J Cancer* 2007 Feb; **43** (3)**:** 617-623.

11. Ebrahimi M, Boldrup L, Coates PJ, Wahlin YB, Bourdon JC, Nylander K. Expression of novel p53 isoforms in oral lichen planus. *Oral Oncol* 2008 Feb; **44** (2)**:** 156-161.

12. Bourdon JC. p53 and its isoforms in cancer. *Br J Cancer* 2007 Aug 6; **97** (3)**:** 277-282.

13. Bourdon JC. p53 and its isoforms in cancer. *Br J Cancer* 2007; **97** (3)**:** 277-282. Epub 2007 Jul 2017.

14. Bourdon JC. p53 Family isoforms. *Curr Pharm Biotechnol* 2007 Dec; **8** (6)**:** 332-336.

15. Anensen N, Oyan AM, Bourdon JC, Kalland KH, Bruserud O, Gjertsen BT. A distinct p53 protein isoform signature reflects the onset of induction chemotherapy for acute myeloid leukemia. *Clin Cancer Res* 2006 Jul 1; **12** (13)**:** 3985-3992.

16. Avery-Kiejda KA, Zhang XD, Adams LJ, Scott RJ, Vojtesek B, Lane DP*, et al.* Small molecular weight variants of p53 are expressed in human melanoma cells and are induced by the DNA-damaging agent cisplatin. *Clin Cancer Res* 2008; **14** (6)**:** 1659-1668. Epub 2008 Feb 1629.

17. Marabese M, Marchini S, Marrazzo E, Mariani P, Cattaneo D, Fossati R*, et al.* Expression levels of p53 and p73 isoforms in stage I and stage III ovarian cancer. *Eur J Cancer* 2008 Jan; **44** (1)**:** 131-141.

18. Fujita K, Mondal AM, Horikawa I, Nguyen GH, Kumamoto K, Sohn JJ*, et al.* p53 isoforms Delta133p53 and p53beta are endogenous regulators of replicative cellular senescence. *Nat Cell Biol* 2009 Sep; **11** (9)**:** 1135-1142.

19. Chen J, Ng SM, Chang C, Zhang Z, Bourdon JC, Lane DP*, et al.* p53 isoform delta113p53 is a p53 target gene that antagonizes p53 apoptotic activity via BclxL activation in zebrafish. *Genes Dev* 2009; **23** (3)**:** 278-290.

20. Bourdon JC, Deguin-Chambon V, Lelong JC, Dessen P, May P, Debuire B*, et al.* Further characterisation of the p53 responsive element--identification of new candidate genes for trans-activation by p53. *Oncogene* 1997; **14** (1)**:** 85-94.

21. Bunz F, Dutriaux A, Lengauer C, Waldman T, Zhou S, Brown JP*, et al.* Requirement for p53 and p21 to sustain G2 arrest after DNA damage. *Science* 1998 Nov 20; **282** (5393)**:** 1497-1501.

22. Courtois S, Verhaegh G, North S, Luciani MG, Lassus P, Hibner U*, et al.* DeltaN-p53, a natural isoform of p53 lacking the first transactivation domain, counteracts growth suppression by wild-type p53. *Oncogene* 2002; **21** (44)**:** 6722-6728.

23. Allan LA, Fried M. p53-dependent apoptosis or growth arrest induced by different forms of radiation in U2OS cells: p21WAF1/CIP1 repression in UV induced apoptosis. *Oncogene* 1999 Sep 23; **18** (39)**:** 5403-5412.

24. Medema RH, Klompmaker R, Smits VA, Rijksen G. p21waf1 can block cells at two points in the cell cycle, but does not interfere with processive DNA-replication or stress-activated kinases. *Oncogene* 1998 Jan 29; **16** (4)**:** 431-441.

25. Juven T, Barak Y, Zauberman A, George DL, Oren M. Wild type p53 can mediate sequence-specific transactivation of an internal promoter within the mdm2 gene. *Oncogene* 1993; **8** (12)**:** 3411-3416.

26. Barak Y, Gottlieb E, Juven-Gershon T, Oren M. Regulation of mdm2 expression by p53: alternative promoters produce transcripts with nonidentical translation potential. *Genes Dev* 1994; **8** (15)**:** 1739-1749.

27. Miyashita T, Harigai M, Hanada M, Reed JC. Identification of a p53-dependent negative response element in the bcl-2 gene. *Cancer Res* 1994; **54** (12)**:** 3131-3135.

28. Bredow S, Juri DE, Cardon K, Tesfaigzi Y. Identification of a novel Bcl-2 promoter region that counteracts in a p53-dependent manner the inhibitory P2 region. *Gene* 2007 Dec 1; **404** (1-2)**:** 110-116.

29. Bourdon JC, Renzing J, Robertson PL, Fernandes KN, Lane DP. Scotin, a novel p53-inducible proapoptotic protein located in the ER and the nuclear membrane. *J Cell Biol* 2002 Jul 22; **158** (2)**:** 235-246.

30. Shaulian E, Haviv I, Shaul Y, Oren M. Transcriptional repression by the C-terminal domain of p53. *Oncogene* 1995; **10** (4)**:** 671-680.

31. Saville MK, Sparks A, Xirodimas DP, Wardrop J, Stevenson LF, Bourdon JC*, et al.* Regulation of p53 by the ubiquitin-conjugating enzymes UbcH5B/C in vivo. *J Biol Chem* 2004 Oct 1; **279** (40)**:** 42169-42181.

32. Stevenson LF, Sparks A, Allende-Vega N, Xirodimas DP, Lane DP, Saville MK. The deubiquitinating enzyme USP2a regulates the p53 pathway by targeting Mdm2. *Embo J* 2007 Feb 21; **26** (4)**:** 976-986.

33. Midgley CA, Fisher CJ, Bartek J, Vojtesek B, Lane D, Barnes DM. Analysis of p53 expression in human tumours: an antibody raised against human p53 expressed in Escherichia coli. *J Cell Sci* 1992; **101** (Pt 1)**:** 183-189.

34. Hoy CA, Carswell C, Schimke RT. Bromodeoxyuridine/DNA analysis of replication in CHO cells after exposure to UV light. *Mutat Res* 1993 Dec; **290** (2)**:** 217-230.

35. Kaeser MD, Iggo RD. Chromatin immunoprecipitation analysis fails to support the latency model for regulation of p53 DNA binding activity in vivo. *Proc Natl Acad Sci U S A* 2002; **99** (1)**:** 95-100. Epub 2001 Dec 2026.

Titles and legends to figures

Figure 1. *Mapping of the promoter activity within intron-4 of the p53 gene*. **(A)** Diagram showing the different *p53* internal promoter deletion constructs (a-f), generated as described in Materials and Methods. Positions of the different restriction enzymes and sizes of the fragments obtained are indicated. Numbers of *p53* introns and exons (empty and shadow boxes respectively) are indicated. **(B)** Basal activity of each *p53* internal promoter deletion construct (a-f). H1299 cells were co-transfected with each of the *p53* internal promoter deletion constructs (a-f) and the Renilla luciferase reporter plasmid. The dual luciferase assay was then performed, as described in Materials and Methods. Each experiment was performed in duplicate and all results shown are the average of at least three separate individual experiments. The promoterless pGL3-basic plasmid was used as a negative control and pBax-luc plasmid was used as a positive control for the luciferase promoter activity. All activities were normalized to pGL3-basic activity.

Figure 2. *Identification and characterization of five p53REs within the p53 internal promoter*. **(A)** Diagram showing the identified p53REs (written in bold and in capital letters within the region of 757-804 bp). Constructs with (a, c) or without (d) the p53REs were generated, as described in Materials and Methods. *p53* introns and exons (empty and shadow boxes respectively) are indicated. (4i) corresponds to intron-4. p53RE region is indicated with a dashed box. **(B)** Induction of the *p53* internal promoter by p53. H1299 cells were co-transfected with each of the *p53* internal promoter constructs (a, c and d) and the p53 expression vector or the empty expression vector PSI. The dual luciferase assay was then performed, each experiment was done in duplicate and all results shown

are the average of at least three separate individual experiments. The p53-inducible *p21* promoter cloned upstream of the luciferase gene was used as a positive control (p21). All luciferase activities were normalized to the basal activity obtained with the empty pSI plasmid and are represented as fold activation. **(C)** Four single point mutations (underlined) were generated within the first two p53REs of the pi3i4-luc construct (Figure 2A, a). WT p53RE and Mutant p53RE sequences are illustrated. H1299 were co-transfected with the pi3i4-luc construct (WT p53RE or Mutant p53RE) and the p53 expression vector or the empty expression vector PSI. The dual luciferase assay was then performed, each experiment was done in duplicate and all results shown are the average of at least three separate individual experiments. All luciferase activities were normalized to the basal activity of the empty pSI plasmid and are represented as fold activation.

Figure 3. *Human p53 internal promoter is directly transactivated by p53.* **(A)** ChIP assay of *p53* internal promoter DNA was carried out by RT-qPCR in MCF7 cells that were left untreated or treated with 60 ng/ml of actinomycin D (Act D) and harvested 2h after treatment, using primers encompassing the p53REs. Exon-8 amplification was performed as a negative control. The amounts of the *p53* internal promoter contained in the input or immunoprecipitated with the DO-1 antibody were quantified by RT-qPCR, as previously described (35). The results are expressed as a percentage of promoter specifically immunoprecipitated by the DO-1 antibody, compared to the total amount of promoter contained in 10% of the input. The results shown are the average of three independent experiments.

(B-E) Quantification of endogenous *p53* internal promoter activity by RT-qPCR in human cancer cells (MCF7, MCF7-DDp53, HCT116-/-, HCT116+/+ and U2OS) or normal human primary fibroblasts (NHDF). **(B)** MCF7 (WTp53) and MCF7-DDp53 (mutant p53) cells were left untreated or treated for 30min, 1h or 2h with 60 ng/ml of Act D and harvested. **(C)** HCT116+/+ (WTp53) and HCT116-/- (devoid of FLp53 expression) cells were left untreated or treated for 1h with 0.5µM of doxorubicin (Doxo) and harvested at the indicated time **(D)** U2OS (WTp53) cells and **(E)** NHDF were left untreated or treated for 1h with 0.5µM of doxorubicin (Doxo) and harvested 24h after treatment. Student t-test was performed and p-values are indicated (the student t-tests were determined by comparing the expression levels of the *p53* internal promoter in cells treated with Act D or doxorubicin, to untreated cells). **, $p<0.01$; ***, $p<0.001$.

For all RT-qPCR experiments, expression levels were normalized to TBP. Results are expressed as the fold change compared to untreated cells and represent mean ± SD of 3 independent experiments.

Figure 4. *Δ133p53α protein is induced in response to doxorubicin treatment.*

(A) HCT116+/+ (p53WT) and HCT116-/- (devoid of FLp53 expression) cells were treated with 0.5µM doxorubicin for 1h and proteins were extracted 24h after treatment in SDS-Laemmli buffer. Western blot analysis was performed using the CM1 rabbit polyclonal antibody which recognizes all p53 isoforms. **(B)** HCT116+/+ transfected for 24h with 50nM of either si133a, si133b (two distinct siRNAs specific for the 5'UTR of Δ133p53 mRNAs) or siNS (non-specific siRNA used as a negative control), were left untreated (-) or treated (+) for 1h with 0.5µM of doxorubicin, as indicated. Proteins were

extracted 24h after treatment and analyzed by western blotting. p53 and its isoforms were revealed with the CM1 antibody. Actin was used as a protein loading control. **(C)** Western blot analysis of endogenous Δ133p53α expression in untreated (-) or doxorubicin-treated (+) NHDF cells. p53 and its isoforms were revealed with the CM1 antibody. Tubulin was used as a protein loading control.

Figure 5. *Δ133p53α antagonizes DNA damage-induced apoptosis and G1 arrest without preventing p53-dependent G2 cell cycle arrest*. U2OS-ctrl and U2OS-Δ133p53 cells were generated after stable transfection with the empty pcDNA3 or the pcDNA3-Δ133p53 expression vectors respectively, as described in Material and Methods. Cells transfected for 24h with 50nM of either si133a, si133b, siTA (siRNA specific for FLp53) or siNS (as indicated), were left untreated (-) or treated (+) for 1h with 0.5µM of doxorubicin, and incubated for a further 24h before harvesting.

Western blot analysis of U2OS-Δ133p53 cells **(A)** and U2OS-ctrl cells **(B)**. p53 and its isoforms were revealed with the CM1 antibody. Tubulin was used as a protein loading control.

(C-E) Cell cycle analysis by flow cytometry after BrdU pulse-labeling of U2OS-ctrl and U2OS-Δ133p53 cells treated as described above. These experiments were carried out in parallel with the western blot analyses described above and a representative BrdU pulse-labeling experiment is shown **(C)**. The average of the percentage of cells in G1 **(D)** and G2 **(E)** are shown.

(F) Apoptosis assay. In parallel to the western blot analyses described above, cells were treated as described above and Annexin V-FITC flow cytometric analysis was carried out. The average of the percentage of apoptotic cells is shown.

Student t-test was performed and p-values are indicated (the student t-tests were carried out by comparing percentages of U2OS-ctrl cells transfected with either si133a, si133b or siTA, to percentages of U2OS-ctrl cells transfected with siNS, after doxorubicin treatment).

All results shown are the average of at least three separate individual experiments.

Figure 6. *Δ133p53α directly interacts with p53 and differentially regulates p21*, *HDM2* and *Bcl-2 expression.* **(A)** Co-Immunoprecipitation of Δ133p53α with p53. H1299 cells were transfected with pSV-p53 and/or pSV-Δ133p53α expression vectors, as indicated. Extracted proteins were immunoprecipitated with the mouse monoclonal antibody DO-1 or with a non-relevant mouse monoclonal IgG antibody, as indicated. DO-1 is specific for FLp53 and does not bind Δ133p53α. Protein content was then analyzed by western blot analysis using the rabbit polyclonal antibody (CM1), recognizing FLp53 and Δ133p53α. 10% of the input was loaded as a control. **(B)** Western blot analysis of p53 target genes (p21, HDM2 and Bcl-2). In parallel to the cell cycle analysis and apoptosis assay, protein extracts from U2OS-ctrl cells treated as described in Figure 5B, were analyzed by western blotting using the corresponding antibodies. Actin was used as a protein loading control.

Titles and legends to supplementary figures

Supplementary Figure A. The *p53* internal promoter may be regulated by numerous transcription factors. List of responsive elements contained in the *p53* internal promoter sequence (1-1555 bp), as analyzed by MatInspector software (V 8.0). The name of the transcription factors, position and sequence of the responsive element are also indicated. Opt: Optimized matrix; Str: DNA strand (+ or -); Core sim.: similarity to the core sequence of a matrix which is defined as the (usually 4) highest conserved, consecutive positions of the matrix, the maximum score for Core sim. is 1; Matrix sim.: similarity to the matrix, the maximum score for Matrix sim. is 1.

Supplementary Figure B. *p53 directly binds and transactivates the p21 promoter.* **(A1)** ChIP assay of *p21* promoter DNA was carried out by RT-qPCR in MCF7 cells that were left untreated or treated for 2h or 6h with 60 ng/ml of actinomycin D (Act D), using primers encompassing the p53REs. The amounts of the *p21* promoter contained in the input or immunoprecipitated with the DO-1 antibody, were quantified by RT-qPCR, as previously described (35). The results are expressed as a percentage of promoter specifically immunoprecipitated by the DO-1 antibody, compared to the total amount of promoter contained in 10% of the input. The results shown are the average of three independent experiments. **(A2)** Quantification of endogenous *p21* promoter activity by RT-qPCR in MCF7 and MCF7-DDp53 cells which were left untreated or treated for 30min, 1h, 2h, 6h or 8h with 60 ng/ml of Act D, as indicated.

For all RT-qPCR experiments, expression levels were normalized to TBP. Results are expressed as the fold change compared to untreated cells and represent mean ± SD of 3 independent experiments.

Supplementary Figure C. *Efficiency of p53 isoforms siRNAs.*

The efficiency of p53 isoforms siRNAs (si133a, si133b and siTA) used in this study was tested by RT-qPCR. **(B1)** Efficiency of Δ133p53 siRNAs (si133a and si133b). **(B2)** Efficiency of siTA (siRNA targeting *p53* mRNAs containing exon-2).

For all RT-qPCR experiments, expression levels were normalized to TBP. Results are expressed as a percentage of cells transfected with siNS and represent mean ± SD of 3 independent experiments.

Supplementary Figure D. *Quantification of p21, HDM2 and Bcl-2 expression by RT-qPCR in U2OS-ctrl cells.*

In parallel to the cell cycle analysis and apoptosis assay, RNA samples from U2OS-ctrl cells treated as described in Figure 5B, were analyzed by RT-qPCR (Taqman). Expression levels were normalized to TBP. Results are expressed relative to the fold change of expression of the p53 target gene in untreated cells transfected with siNS and represent mean ± SD of 3 independent experiments.

Student t-test was performed and p-values are indicated (the student t-tests were carried out by comparing the expression levels of the p53 target gene in U2OS-ctrl cells transfected with either si133a, si133b or siTA, to U2OS-ctrl cells transfected with siNS, after doxorubicin treatment).

All results shown are the average of at least three separate individual experiments.

Table 1. *PCR primers used for cloning, ChIP and RT-qPCR assays.*

Primers for cloning and mutagenesis of the *p53* internal promoter
p53RE-a fwd: 5’ ACAGGAGGTGGGAGCAGGGCACGGTA 3’
p53RE-a rev: 5’ GTTGGCAAAACATCTTGTTGAGGGC 3’
p53RE-b fwd: 5’AAAACCTACCAGGGCAGCTACGGT 3’
p53RE-c fwd: 5’ GGAACTTTGGGATTCCTCTTCACCCTTA 3’
Mut-p53RE fwd: 5’ CTGGGACAGCAAAATCTGTCACGTGCACGGTCAG 3’
Mut-p53RE rev: 5’ CTGACCGTGCACGTGACAGATTTTGCTGTCCCAG 3’
Primers for ChIP assay on the *p53* internal promoter
Chip-p53RE fwd: 5’ CAGGGCAGCTACGGTTTCC 3’
Chip-p53RE rev: 5’ GCAACTGACCGTGCAAGTCA 3’
Chip-p53RE probe: Fam- 5’ TGCATTCTGGGACAGCCAAGTC 3’-Tamra
Chip-Exon8 fwd: 5’ GAATCTCCGCAAGAAAGG 3’
Chip-Exon8 rev: 5’ TTGCTTACCTCGCTTAGTG 3’
Chip-Exon8 probe: Fam- 5’ CTCACCACGAGCTGCCCCCAG 3’-Tamra
Primers for RT-qPCR
mRNA-p53RE fwd: 5’ ACTCTGTCTCCTTCCTCTTCCTACAG3’
mRNA-p53RE rev: 5’ GTGTGGAATCAACCCACAGCT 3’
mRNA-p53RE probe: Fam- 5’ TCCCCTGCCCTCAACAAGATGTTTTGCC 3’-Tamra
mRNA-TBP fwd: 5’ CACGAACCACGGCACTGATT 3’
mRNA- TBP rev: 5’ TTTTCTTGCTGCCAGTCTGGAC 3’
mRNA- TBP probe: Fam- 5’TGTGCACAGGAGCCAAGAGTGAAGA 3’-Tamra

A

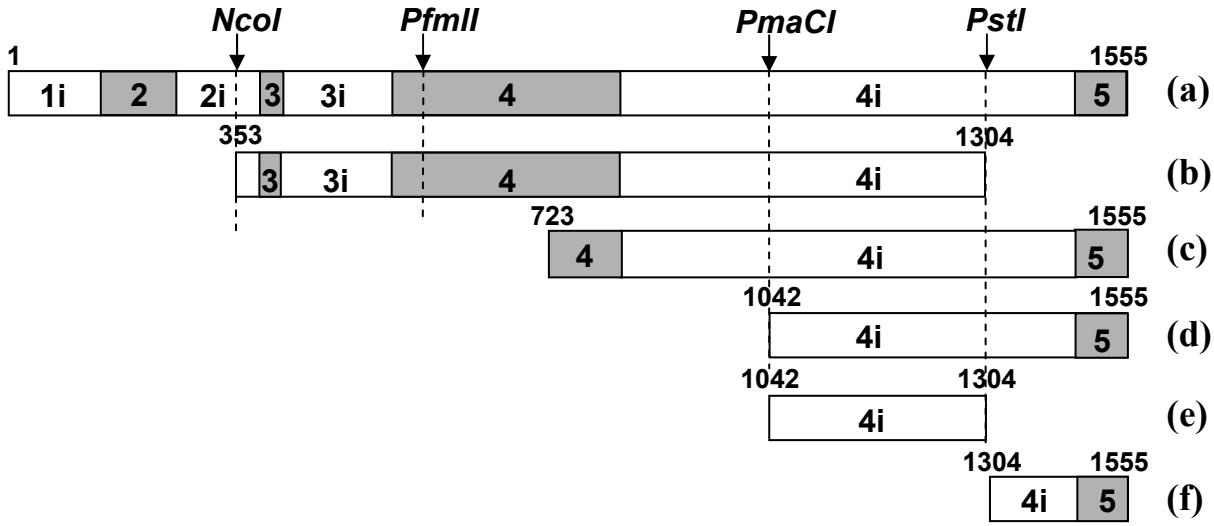
NcoI
PfmlI
PmaCI
PstI
1
1555
1i
2
2i
3
3i
4
4i
5
(a)
353
1304
(b)
723
(c)
1042
(d)
(e)
(f)

B

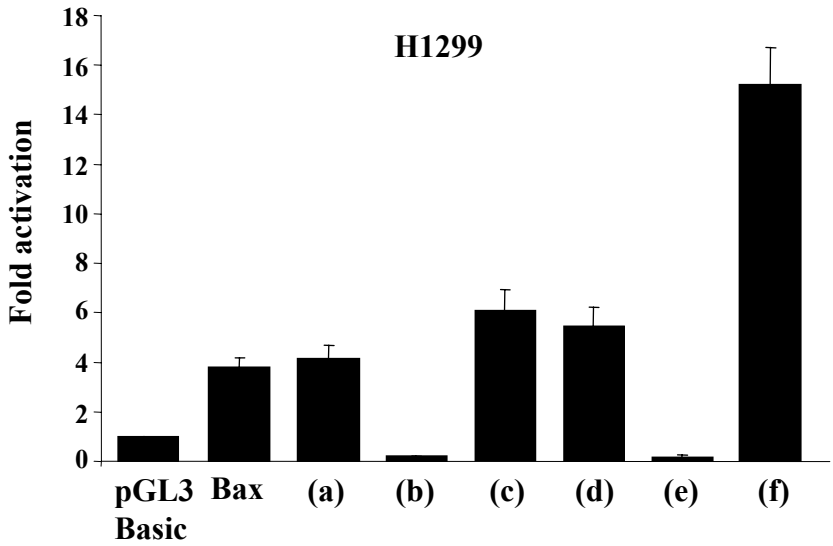
H1299
Fold activation
18
16
14
12
10
8
6
4
2
0
pGL3 Basic
Bax
(a)
(b)
(c)
(d)
(e)
(f)

A

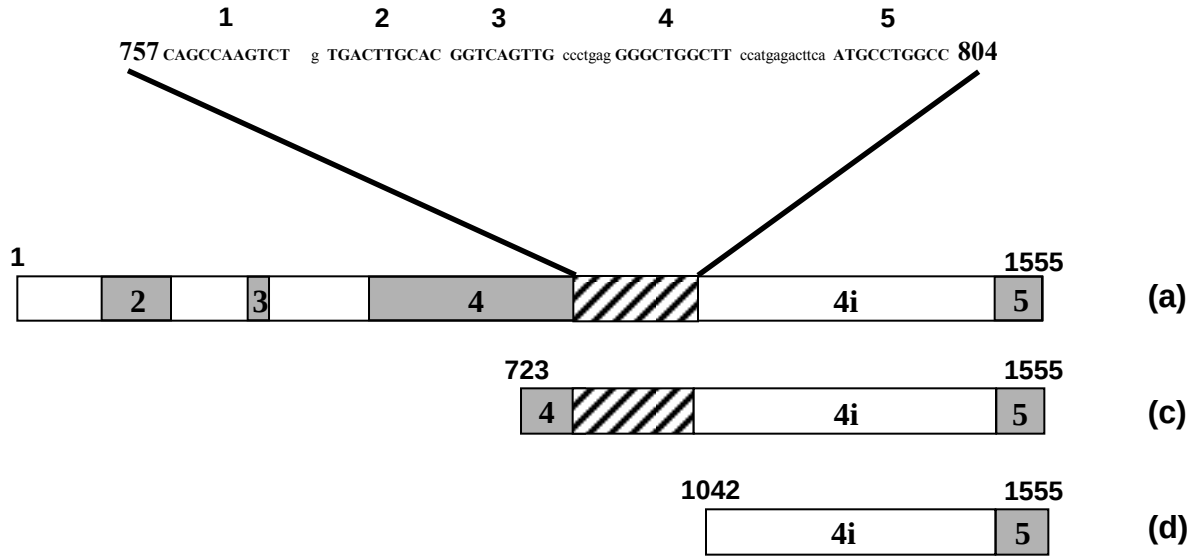
1
2
3
4
5
757 CAGCCAAGTCT g TGACTTGCAC GGTCAGTTG cctgag GGGCTGGCTT ccatgagacttca ATGCCTGGCC 804
1
1555
2
3
4
4i
5
(a)
723
1555
4
4i
5
(c)
1042
1555
4i
5
(d)

B

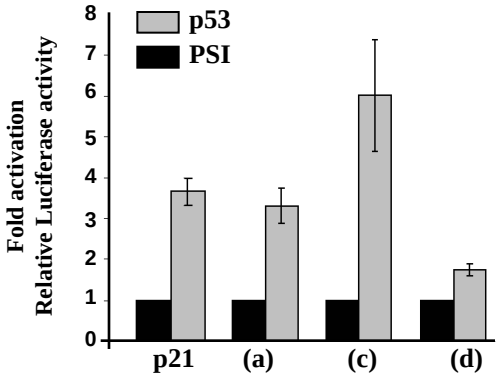
p53
PSI
Fold activation
Relative Luciferase activity
0
1
2
3
4
5
6
7
8
p21
(a)
(c)
(d)

C


1
2
3
4
5
WT p53RE 757 CAGCCAAGTCT G TGACTTGCAC GGTCAGTTG CCCTGAG GGGCTGGCTT CCATGAGACTTCA ATGCCTGGCC 804
Mutant p53RE 757 CAGCAAAATCT G TCACGTGCAC GGTCAGTTG CCCTGAG GGGCTGGCTT CCATGAGACTTCA ATGCCTGGCC 804

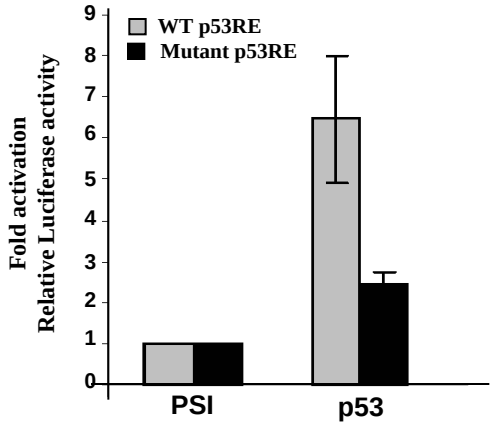
WT p53RE
Mutant p53RE
Fold activation
Relative Luciferase activity
0
1
2
3
4
5
6
7
8
9
PSI
p53

A

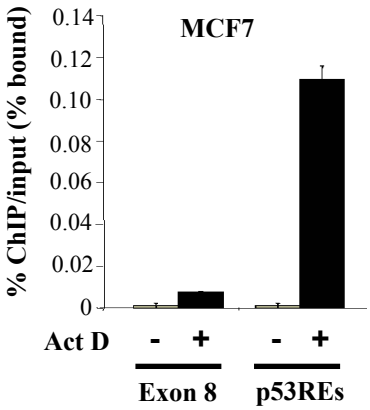
MCF7
% ChIP/input (% bound)
0.14
0.12
0.10
0.08
0.06
0.04
0.02
0
Act D - + - +
Exon 8
p53REs

B

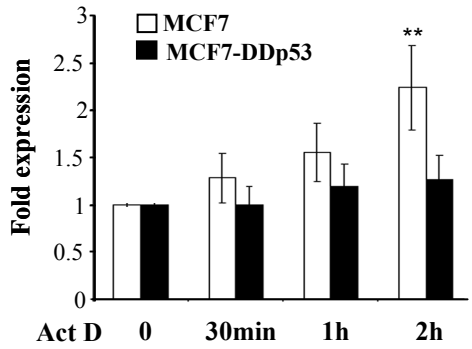
MCF7
MCF7-DDp53
Fold expression
3
2.5
2
1.5
1
0.5
0
**
Act D 0 30min 1h 2h

C

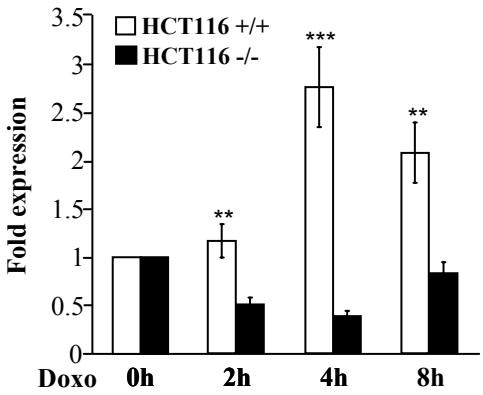
HCT116 +/+
HCT116 -/-
Fold expression
3.5
3
2.5
2
1.5
1
0.5
0
**
***
**
Doxo 0h 2h 4h 8h

D

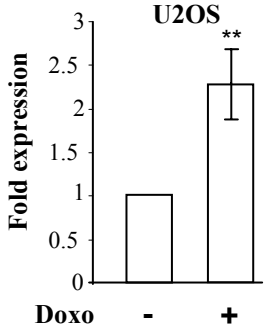
U2OS
Fold expression
3
2.5
2
1.5
1
0.5
0
**
Doxo - +

E

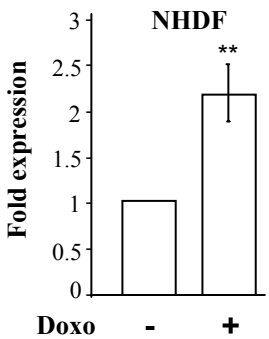
NHDF
Fold expression
3
2.5
2
1.5
1
0.5
0
**
Doxo - +

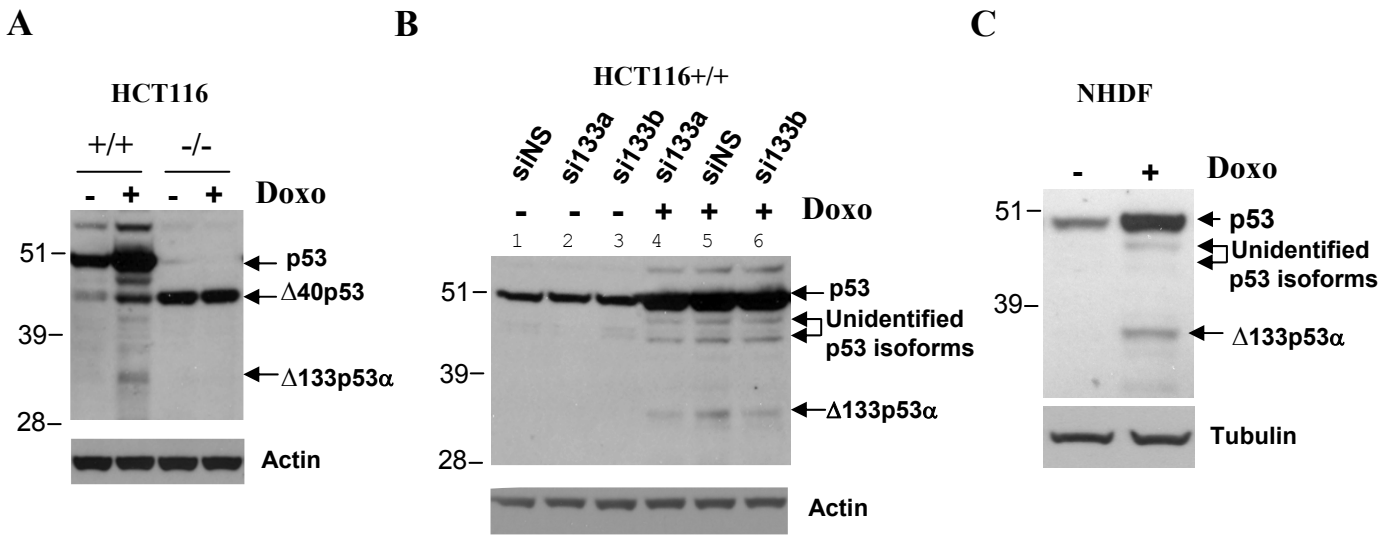
A
HCT116
+/+
-/-
- + - +
Doxo
51–
39–
28–
p53
Δ40p53
Δ133p53α
Actin
B
HCT116+/+
siNS
si133a
si133b
si133a
siNS
si133b
- - - + + +
Doxo
1 2 3 4 5 6
51–
39–
28–
p53
Unidentified
p53 isoforms
Δ133p53α
Actin
C
NHDF
- +
Doxo
51–
39–
p53
Unidentified
p53 isoforms
Δ133p53α
Tubulin

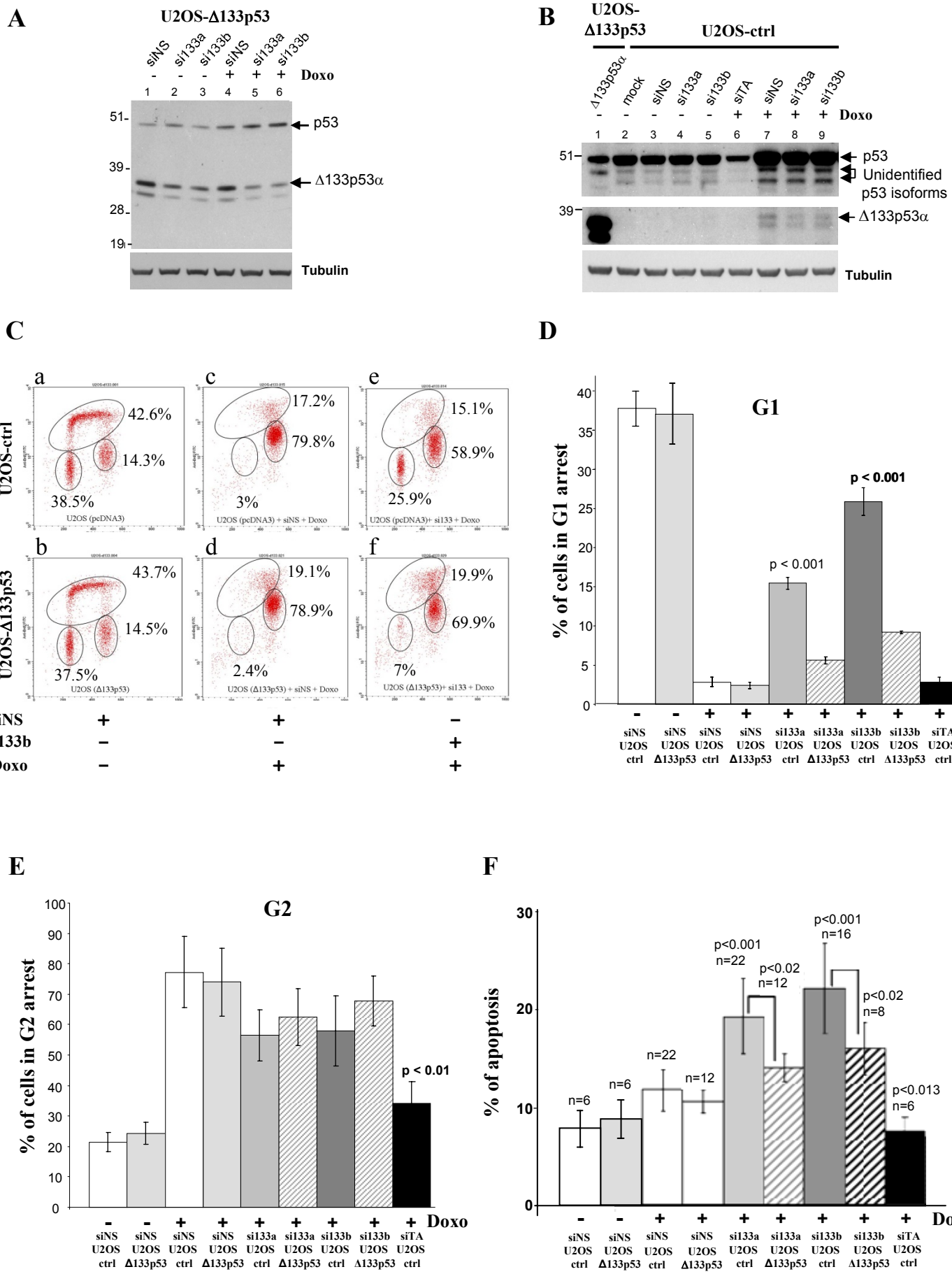
A
U2OS-Δ133p53
siNS
si133a
si133b
siNS
si133a
si133b
- - - + + + Doxo
1 2 3 4 5 6
51
39
28
19
p53
Δ133p53α
Tubulin
B
U2OS-Δ133p53
U2OS-ctrl
Δ133p53α
mock
siNS
si133a
si133b
siTA
siNS
si133a
si133b
- - - - - + + + + Doxo
1 2 3 4 5 6 7 8 9
51
39
p53
Unidentified p53 isoforms
Δ133p53α
Tubulin
C
a
c
e
b
d
f
U2OS-ctrl
U2OS-Δ133p53
42.6%
14.3%
38.5%
U2OS (peDNA3)
17.2%
79.8%
3%
U2OS (peDNA3) + siNS + Doxo
15.1%
58.9%
25.9%
U2OS (peDNA3)+ si133 + Doxo
43.7%
14.5%
37.5%
U2OS (Δ133p53)
19.1%
78.9%
2.4%
U2OS (Δ133p53) + siNS + Doxo
19.9%
69.9%
7%
U2OS (Δ133p53)+ si133 + Doxo
siNS + - +
si133b - - +
Doxo - + +
D
G1
% of cells in G1 arrest
p < 0.001
p < 0.001
siNS U2OS ctrl
siNS U2OS Δ133p53
siNS U2OS ctrl
siNS U2OS Δ133p53
si133a U2OS ctrl
si133a U2OS Δ133p53
si133b U2OS ctrl
si133b U2OS Δ133p53
siTA U2OS ctrl
E
G2
% of cells in G2 arrest
p < 0.01
Doxo
siNS U2OS ctrl
siNS U2OS Δ133p53
siNS U2OS ctrl
siNS U2OS Δ133p53
si133a U2OS ctrl
si133a U2OS Δ133p53
si133b U2OS ctrl
si133b U2OS Δ133p53
siTA U2OS ctrl
F
% of apoptosis
n=6
n=6
n=22
n=12
p<0.001 n=22
p<0.02 n=12
p<0.001 n=16
p<0.02 n=8
p<0.013 n=6
Doxo
siNS U2OS ctrl
siNS U2OS Δ133p53
siNS U2OS ctrl
siNS U2OS Δ133p53
si133a U2OS ctrl
si133a U2OS Δ133p53
si133b U2OS ctrl
si133b U2OS Δ133p53
siTA U2OS ctrl

A

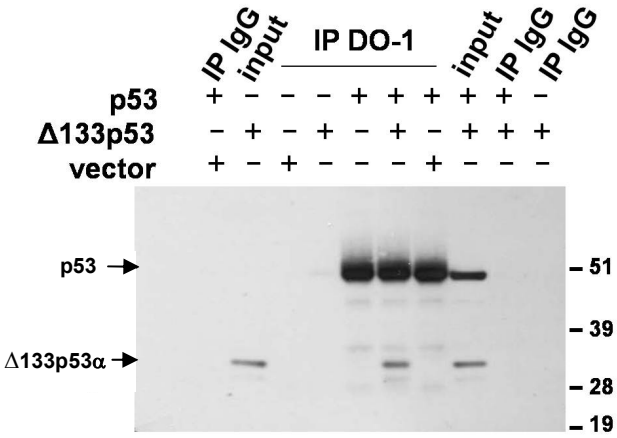
IP IgG
input
IP DO-1
input
IP IgG
IP IgG
p53
Δ133p53
vector
p53
Δ133p53α
51
39
28
19

B

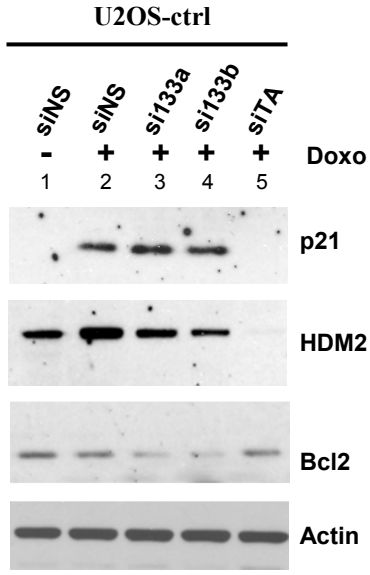
U2OS-ctrl
siNS
siNS
si133a
si133b
siTA
Doxo
1
2
3
4
5
p21
HDM2
Bcl2
Actin

Family/matrix	Further Information	Opt.	Position from - to	Str.	Core sim.	Matrix sim.	Sequence (red: ci-value > 60 capitals: core sequence)
V$ZNFP/ZBRK1.01	Transcription factor with 8 central zinc fingers and an N-terminal KRAB domain	0.77	17 - 41	(+)	1.000	0.784	aatgtgaaGCAGccattcttttcct
V$ETSF/ETS2.01	c-Ets-2 binding site	0.84	28 - 48	(-)	1.000	0.866	gtggagcAGGAaaagaatggc
V$ETSF/CETS1P54.01	c-Ets-1(p54)	0.92	42 - 62	(+)	0.901	0.948	gctccaCAGGaagccgagctg
V$ZBPF/ZNF219.01	Kruppel-like zinc finger protein 219	0.91	74 - 96	(-)	1.000	0.967	ggcccctCCCCcaacaccatgcc
V$ZBPF/ZBP89.01	Zinc finger transcription factor ZBP-89	0.93	77 - 99	(-)	1.000	0.989	ggaggcccctCCCCcaacaccat
V$EREF/ER.01	Estrogen receptor, IR3 sites	0.83	106 - 124	(-)	1.000	0.831	ctggGTCAcctgggcctgc
V$EBOX/USF.04	Upstream stimulating factor 1/2	0.90	110 - 122	(-)	0.829	0.935	gggtCACCtgggc
V$AP1F/AP1.03	Activator protein 1	0.94	235 - 245	(+)	1.000	0.978	tcTGAGtcagg
V$ETSF/ETS2.01	c-Ets-2 binding site	0.84	236 - 256	(+)	1.000	0.920	ctgagtcAGGAaacattttca
V$IRFF/IRF3.01	Interferon regulatory factor 3 (IRF-3)	0.85	337 - 357	(+)	1.000	0.850	tgtgggaagcGAAAattcatg
V$E2FF/E2F.01	E2F, involved in cell cycle regulation, interacts with Rb p107 protein	0.75	338 - 354	(+)	1.000	0.758	gtgggaagcGAAAattc
V$ETSF/CETS1P54.01	c-Ets-1(p54)	0.92	379 - 399	(-)	0.901	0.949	tgttttCAGGaagtctgaaag
V$HEAT/HSF1.01	Heat shock factor 1	0.84	379 - 403	(-)	0.952	0.859	acgttgttttcaGGAAgtctgaaag
V$STAT/STAT.01	Signal transducers and activators of transcription	0.87	382 - 400	(-)	1.000	0.911	ttgttttcaGGAAgtctga
V$STAT/STAT6.01	STAT6: signal transducer and activator of transcription 6	0.84	384 - 402	(+)	1.000	0.846	agacTTCCtgaaaacaacg
V$FKHD/FKHRL1.01	Fkh-domain factor FKHRL1 (FOXO)	0.83	388 - 404	(+)	1.000	0.874	ttcctgaaAACAacgtt
V$HEAT/HSF1.01	Heat shock factor 1	0.84	394 - 418	(-)	1.000	0.874	cttgtccttaccAGAAcgttgtttt
V$ZBPF/ZNF219.01	Kruppel-like zinc finger protein 219	0.91	432 - 454	(-)	1.000	0.985	cccagccCCCCcagccctccagg
V$STAT/STAT5.01	STAT5: signal transducer and activator of transcription 5	0.89	560 - 578	(+)	0.845	0.900	atggTTCActgaagaccca
V$HIFF/HIF1.02	Hypoxia inducible factor, bHLH / PAS protein family	0.93	613 - 625	(+)	1.000	0.934	ctccccgCGTGgc
V$EBOX/NMYC.01	N-Myc	0.92	614 - 626	(+)	1.000	0.933	tccccgCGTGgcc
V$ETSF/ELK1.02	Elk-1	0.91	720 - 740	(-)	1.000	0.912	gcccagacGGAAaccgtagct
V$ZFHX/AREB6.04	AREB6 (Atp1a1 regulatory element binding factor 6)	0.98	722 - 734	(+)	1.000	0.988	ctacgGTTTccgt
V$SMAD/SMAD3.01	Smad3 transcription factor involved in TGF-beta signaling	0.99	733 - 741	(+)	1.000	0.993	GTCTgggct
V$P53F/P53.05	Tumor suppressor p53	0.78	757 - 779	(+)	1.000	0.866	cagcCAAGtctgtgacttgcacg
V$HOXF/NANOG.01	Homeobox transcription factor Nanog	0.94	913 - 929	(+)	1.000	0.949	cacttAATGtgtgatct
V$RXRF/RXR_RXR.01	Retinoid X receptor homodimer, DR1 sites	0.78	916 - 940	(-)	0.888	0.904	acaggagtcagaGATCacacattaa
V$CLOX/CDP.02	Transcriptional repressor CDP	0.81	971 - 989	(+)	0.795	0.868	gggcttttATCCatcccat
V$EBOX/NMYC.01	N-Myc	0.92	1037 - 1049	(+)	1.000	0.990	catccaCGTGtat
V$EBOX/USF.01	Upstream stimulating factor	0.87	1038 - 1050	(-)	1.000	0.983	aataCACGtggat
V$RBPF/RBPJK.02	Mammalian transcriptional repressor RBP-Jkappa/CBF1	0.94	1264 - 1278	(+)	1.000	0.963	gaggTGGGaagatca
V$LEFF/LEF1.01	TCF/LEF-1, involved in the Wnt signal transduction pathway	0.86	1451 - 1467	(-)	1.000	0.870	acggcagCAAAgaaaca

A1

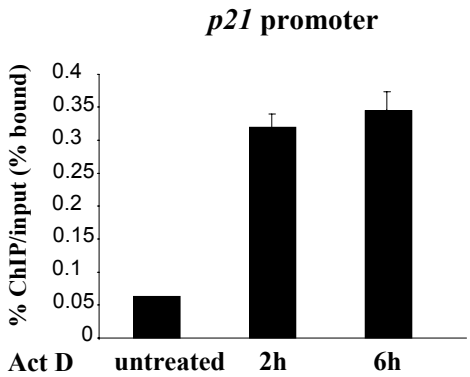
p21 promoter
% ChIP/input (% bound)
0.4
0.35
0.3
0.25
0.2
0.15
0.1
0.05
0
Act D
untreated
2h
6h

A2

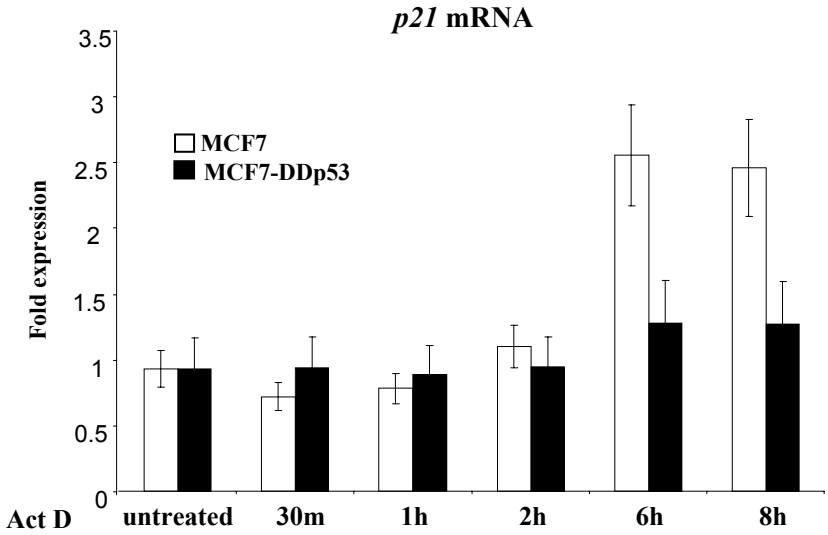
p21 mRNA
Fold expression
3.5
3
2.5
2
1.5
1
0.5
0
MCF7
MCF7-DDp53
Act D
untreated
30m
1h
2h
6h
8h

B1

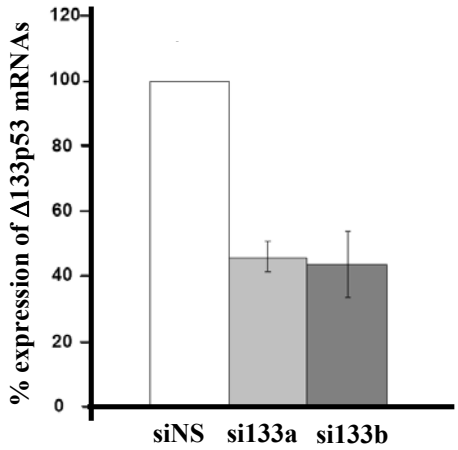
% expression of Δ133p53 mRNAs
120
100
80
60
40
20
0
siNS
si133a
si133b

B2

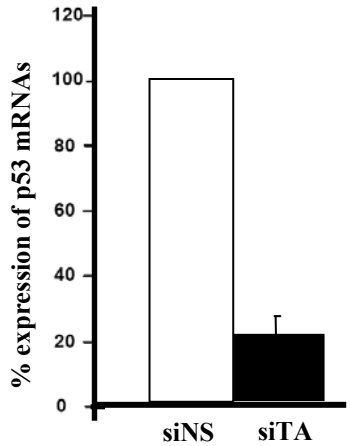
% expression of p53 mRNAs
120
100
80
60
40
20
0
siNS
siTA

C U2OS-ctrl

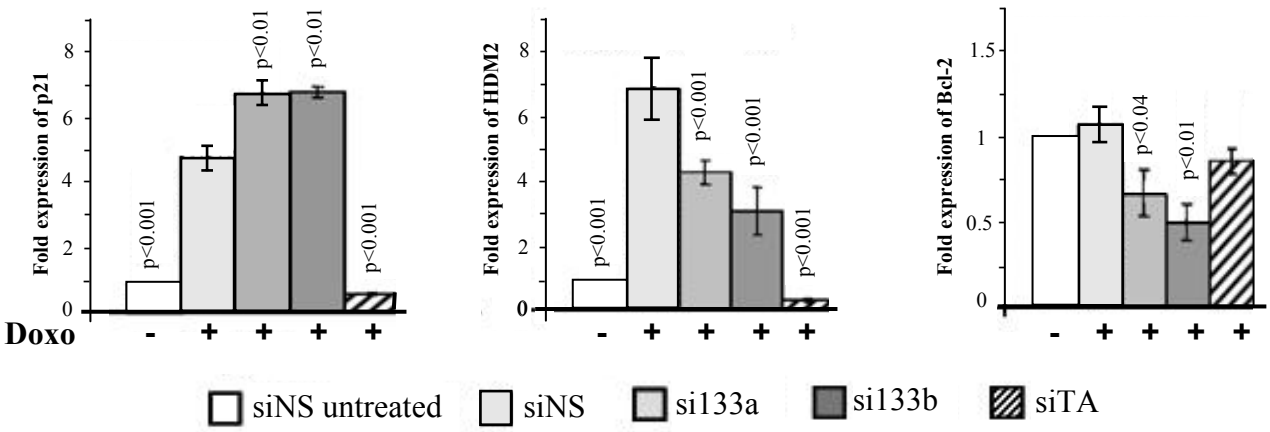
Fold expression of p21
8
6
4
2
0
p<0.001
p<0.01
p<0.01
p<0.001
Doxo
- + + + +
Fold expression of HDM2
8
6
4
2
0
p<0.001
p<0.001
p<0.001
p<0.001
- + + + +
Fold expression of Bcl-2
1.5
1
0.5
0
p<0.04
p<0.01
- + + + +
siNS untreated
siNS
si133a
si133b
siTA